CHEUNG Ho Nam
Department of Physics & Materials Science, City University of Hong Kong, Hong Kong, China
Wen ZHOU
Guy Carpenter Asia-Pacific Climate Impact Center, City University of Hong Kong, Hong Kong, China

Interdecadal Variation of Winter Monsoon over South China

Abstract

South China situates at the boundary between the Eurasian continent and South China Sea, which is part of East Asian monsoon region. In northern winter (December-February, DJF), cold surges often approach there resulting in significant drop of air temperature. However, their strength is usually weak when they arrive there. Since the specific heat capacity of the ocean is much larger than the land, the cold surges normally have smaller effect on South China Sea. In this study, the cold surge variations and the corresponding mechanisms for these geographical regions are explored on decadal timescales.

Wavelet analysis is adopted to study winter monsoon variations. Data are collected from NCEP-NCAR reanalysis dataset and six local weather stations. Based on the gridding of the reanalysis dataset, South China is divided into three regions, which are (1) continent, (2) land-ocean boundary and (3) ocean. It is found that winter monsoon over South China might undergo interdecadal variation with dominant period around 32-64 years. It is also found that the continent part of South China might have teleconnections with Pacific Decadal Oscillation (PDO) and North Atlantic Oscillation (NAO) while the ocean part of South China might have teleconnections with El Niño/Southern Oscillation (ENSO).

1. Introduction

Many studies showed the linkage between East Asian winter monsoon and El Niño/Southern Oscillation (ENSO) (e.g. *Li*, 1990; *Zhang et al.*, 1996). However, recent studies pinpointed this relationship had changed since middle 1970s (e.g. *Chang et al.* 2000, *Zhou et. al,* 2007). Zhou et. al. (2007) pointed out this changing relationship was related to the phase relationship between ENSO and PDO, where PDO (Pacific Decadal Oscillation) is an El Niño like interdecadal oscillation that shifts every 20-30 years (e.g. *Mantua et al.*, 1997). On the other hand, the origin of cold-air mass in this monsoon region is a cold-core pressure system known as Siberian High. The multi-decadal oscillation in North Atlantic Ocean called North Atlantic Oscillation (NAO) has been found to have great influence on temperature over Siberia in winter (e.g. *Hurrel et. al.*, 2003). Hence, ENSO, PDO and NAO may influence the intensity of cold surges from Siberian High. Being part of East Asian monsoon region, South China is under the influence of cold surges originating from the High. This study tries to explore their contribution on interdecadal variations of winter monsoon over South China.

Annual mean winter air temperature is used for studying the variations of winter monsoon. The study is conducted by considering both continent and ocean part of South China. Apart from the intensity of cold surge, the frequency

of cold surge arriving South China is another factor affecting the temperature throughout a winter. The frequency depends on sea level pressure difference between Siberian High and South China. The relationship between this difference and temperature in South China will also be studied.

In this paper, sources of data are presented in section 2. Then, interdecadal variations of winter monsoon over South China are described in section 3 and the corresponding possible mechanisms are described in section 4. At the end, there is a summary of the findings in section 5.

2. Data

Air temperature and sea level pressure data of each region are collected from NCEP-NCAR reanalysis dataset. Air temperature data are also collected from six cities. The boundary condition of the three regions and source of data are summarized in Table 5-1 and Table 5-2 respectively. The Siberian High of this project is defined as sea level pressure averaged over 40-60°N, 70-120°E based on the data from NCEP-NCAR reanalysis dataset between 1948 and 2007. ENSO and PDO indices are collected from Joint Institute for the Study of the Atmosphere and Ocean (JISAO) while NAO index is collected from Climate Research Unit (CRU), University of East Anglia, Norwich, U.K. The sources of three datasets are summarized in Table 5-3.

3. Interdecadal variations of winter monsoon over South China

It is not efficient to analyze every temperature dataset, so correlation analysis is adopted to reduce the number of datasets to be analyzed. The correlations among all unfiltered temperature datasets used in this project are summarized in Table 5-4. NCEP R1/R2/R3 represents the NCEP-NCAR gridded region 1/2/3 in this project.

Data from Macao and Hong Kong are reasonable to generalize the variations of temperature in the continent part of South China. The lowest correlation among all local cities is 0.832 between Shaoguan and Shanwei. Since the null hypothesis of no correlation between them having 53 degrees of freedom (DOF) is true only for correlation smaller than 0.323 for the right-tailed test at the 0.01 level of significance, the two cities are highly correlated. Other correlations between any 2 cities for null hypothesis are equal or smaller since their DOF are equal or larger than 53, so all cities are highly correlated. Macao has the longest continuous temperature record in South China while Hong Kong has the earliest temperature record among all datasets. The temperature of Macao and Hong Kong can describe the general features of South China with very high confidence. Similarly, data from NCEP-NCAR gridded region 1 can accurately describe the characteristics of the land and coastal cities in South China. The wavelet power spectrum and reconstructed time series of Macao are shown in Figure 5-1.

Interdecadal variation of air temperature in the continent part of South China can be separated to six stages from 1885 onwards. Firstly, the air temperature is generally below-normal in late 1880s and 1890s; secondly, it is close to normal between early 1900s and middle 1910s where above-normal events are slightly more; thirdly, it is generally below-normal between middle 1910s and middle 1930s where the it is sometimes above-normal in 1920s; fourthly, it is often above-normal between late 1930s and early 1950s; fifthly, it is generally below-normal between middle 1950s and late 1980s; lastly, above-normal events are dominant afterwards.

The ocean portion of South China (South China Sea) somehow behaves differently with the continent part. From Table 5-4, two

observations show that the coastal cities of South China behave more likely as the land region than the ocean region. Firstly, the correlation between the adjacent NCEP gridded regions, i.e. between NCEP R1 and R2 and between NCEP R2 and R3 (~0.9), is fairly higher than that separated by one region, i.e. between NCEP R1 and R3 (~0.7). Secondly, the local cities in both region 1 and 2 is most correlated with NCEP R1 among the three NCEP gridded regions. Since NCEP R2 encloses much more ocean area than land area compared with the cities at the land-sea contrast, the average temperature of this gridded region is less affected by the cold surge.

Since the correlation between NCEP R2 and NCEP R3 is very high (0.908) and NCEP R3 is purely ocean region, it is reasonable to use NCEP R3 to represent the interdecadal variation of cold surge in the ocean part of South China. The wavelet power spectrum of NCEP R3 is given in Figure 5-2.

The winter monsoon of the ocean part of South China shows similar interdecadal variation as the continent part since 1950s. To begin with, above-normal events seem to be dominant before middle 1950s. After that, below-normal events are dominant between middle 1950s and late 1980s. Then, above-normal events are dominant again since late 1980s. However, the length of data available from NCEP-NCAR reanalysis dataset is too short to describe interdecadal variation.

In short, interdecadal variation of winter monsoon in continent part and ocean part of South China may have similar pattern. The primary period might be around 32-64 years in the 20th century. As the length of data for the ocean part of South China is only 59 years (1949-2007), it is inadequate to arrive at this conclusion under the constraint of Nyquist frequency.

4. *Possible mechanisms*

Even though the winter monsoon variations of the continent and ocean portion of South China might be similar after 1950s, the two regions might have different possible mechanisms. Siberian High, Sea level pressure difference between Siberian High and South China (SLP (SMH-SC)), ENSO, PDO and NAO altogether may construct the possible mechanism for interdecadal variation of winter monsoon of the two regions. They all may have moderate or significant powers for the period around 32-64 years (not shown).

Firstly, SLP (SMH-SC) shows different correlations with air temperature in South China for the two regions. SLP (SMH-SC) has very weak correlations before 1980s with the temperature. Afterwards, the correlations are negative, which are strongest in region 1 (the continent part) and weakest in region 3 (Central South China Sea) (Figure 5-3).

Secondly, air temperature in the continent portion and the ocean portion shows different relationship with ENSO and PDO (Figure 5-4). The temperature in the continent part* has positive correlation with both ENSO and PDO before 1930s but the correlation becomes weak afterward. The temperature in the ocean part, on the other hand, has positive correlation with ENSO before late 1980s but no correlation with PDO for all time. Meanwhile, the correlation between ENSO and PDO is quite high. Therefore, PDO may not have direct teleconnections with the winter air temperature in South China while ENSO may have direct teleconnections with the temperature in ocean part of South China.

*Note that Macao is used for the substitute for NCEP gridded region 1 because Macao has longest continuous data and the two datasets have high correlation (Table 5-4).

Thirdly, PDO has much stronger correlation with the SLP over Siberian High than ENSO

Region	Gridded data from NCEP-NCAR	Local weather station
1 Continent part of South China	22.5-25.0°N, 112.5-115.0°E	Guangzhou (23.17°N, 113.3°E)
		Shaoguan (24.68°N, 113.6°E)
		Heyuan (23.73°N, 114.7°E)
2 Northern South China Sea and Coastal area of South China	20.0-22.5°N, 112.5-115.0°E	Hong Kong (22.30°N, 114.2°E)
		Macao (22.20°N, 113.5°E)
		Shanwei (22.80°N, 115.4°E)
3 Central South China Sea	17.5-20.0°N, 112.5-115.0°E	Nil

Table 5-1: Grids of three selected regions in South China using NCEP-NCAR reanalysis dataset and six cities

Name of Organization	Acronym	Year of record	Official website
China Meteorological Administration	CMA	1951 – 2007	http://www.cma.gov.cn/
Hong Kong Observatory	HKO	1884 – 1941 1947 – 2007	http://www.hko.gov.hk/
Macao Meteorological and Geophysical Bureau	SMG	1901 – 2007	http://www.smg.gov.mo/
National Center for Environmental Prediction	NCEP	1948 – 2007	http://www.cdc.noaa.gov/

Table 5-2: Source of meteorological data in South China

Dataset	Earliest record	Year of record used in this project	Website
ENSO index	1817	1850-2007	http://jisao.washington.edu/datasets/globalsstenso/
PDO index	1901	1901-2007	http://jisao.washington.edu/pdo/
NAO index	1821	1850-2007	http://www.cru.uea.ac.uk/~timo/projpages/nao_update.htm

Table 5-3: Source of ENSO, PDO and NAO indices

Correlation(r)	NCEP R1	NCEP R2	NCEP R3	Guangzhou	Heyuan	Shaoguan	Hong Kong	Macao	Shanwei
NCEP R1	1								
NCEP R2	0.907	1							
NCEP R3	0.693	0.908	1						
Guangzhou	0.861	0.813	0.677	1					
Heyuan	0.843	0.779	0.683	0.956	1				
Shaoguan	0.835	0.702	0.553	0.898	0.912	1			
Hong Kong	0.831	0.782	0.698	0.895	0.939	0.863	1		
Macao	0.868	0.797	0.633	0.944	0.910	0.887	0.938	1	
Shanwei	0.882	0.886	0.784	0.947	0.923	0.832	0.949	0.942	1

Table 5-4: Correlations among unfiltered data from NCEP-NCAR and local stations

(a) Wavelet power spectrum

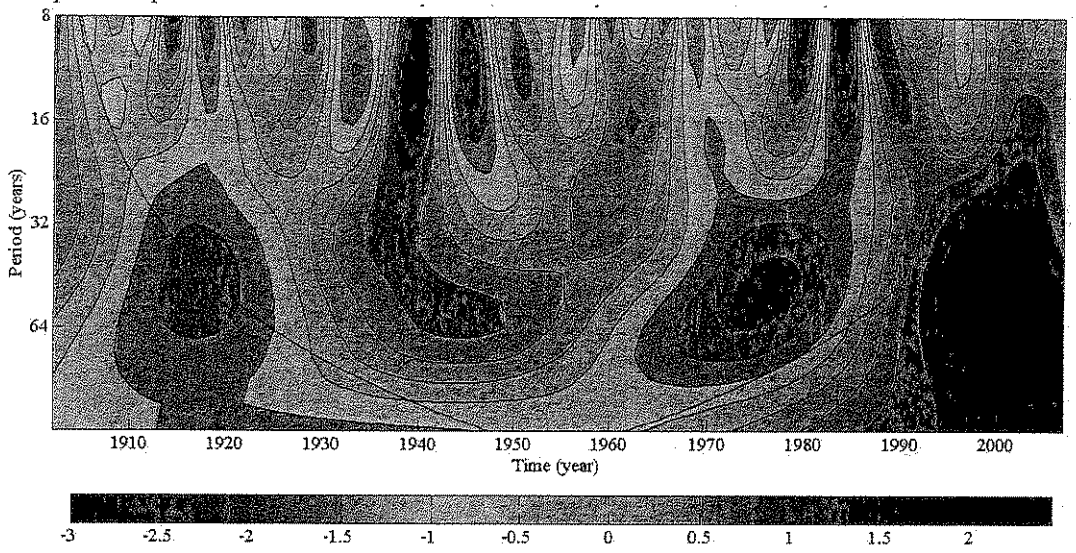

(b) Reconstructed time series

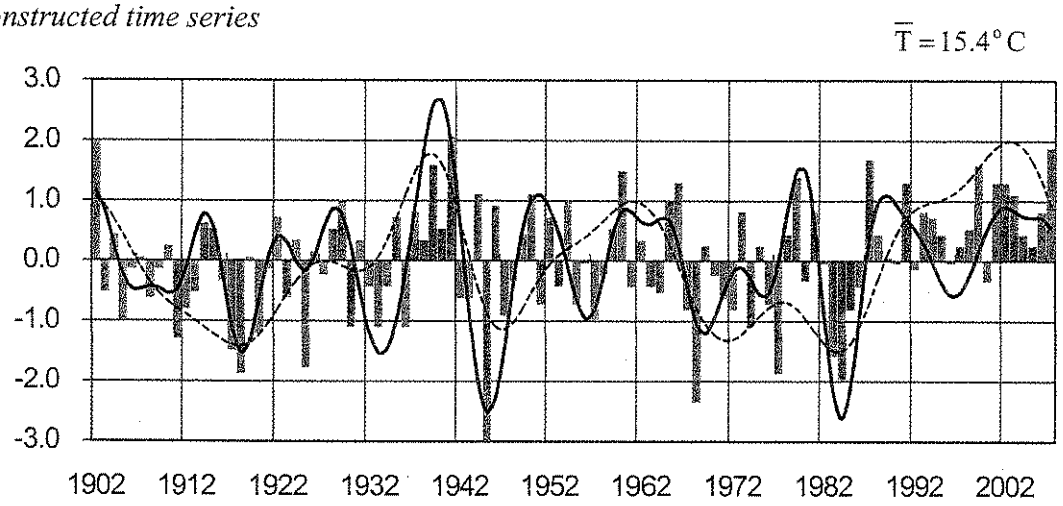

Figure 5-1 Interdecadal variation of winter mean air temperature in Macao (1902-2007): (a) Wavelet power spectrum of the region using the Mexican hat wavelet (derivate of Gaussian; DOG m=2) and; (b) the anomalies of interannual data and reconstructed time series of the city, where the anomalies are represented by the bars, the timescale 8-16 year is represented by the solid line and that of 16-32 year is represented by the dashed line. Note that the long-term mean temperature of each dataset is shown at the top right hand corner of graph (b). The thick black curve in the spectrum indicates edge effects

(a) Wavelet power spectrum

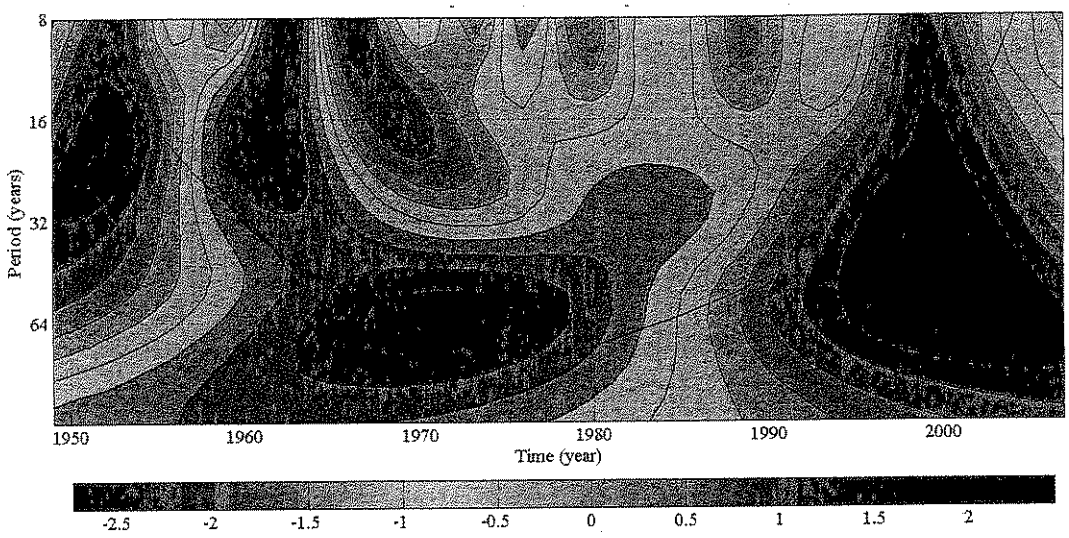

(b) Reconstructed time series

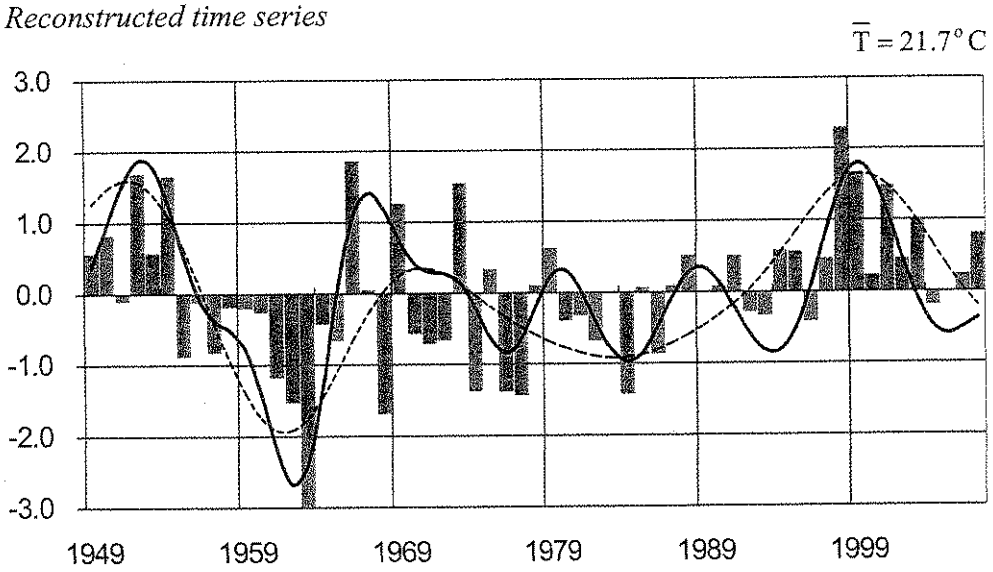

Figure 5-2 Interdecadal variation of winter mean air temperature in region 3 using NCEP-NCAR reanalysis dataset (1949-2007): (i) Wavelet power spectrum of the region and; (ii) the anomalies of interannual data and reconstructed time series of the region, where the anomalies are represented by the bars, the timescale 8-16 year is represented by the solid line and that of 16-32 year is represented by the dashed line. Note that the long-term mean winter air temperature of each area is shown at the top right hand corner of graph (ii).

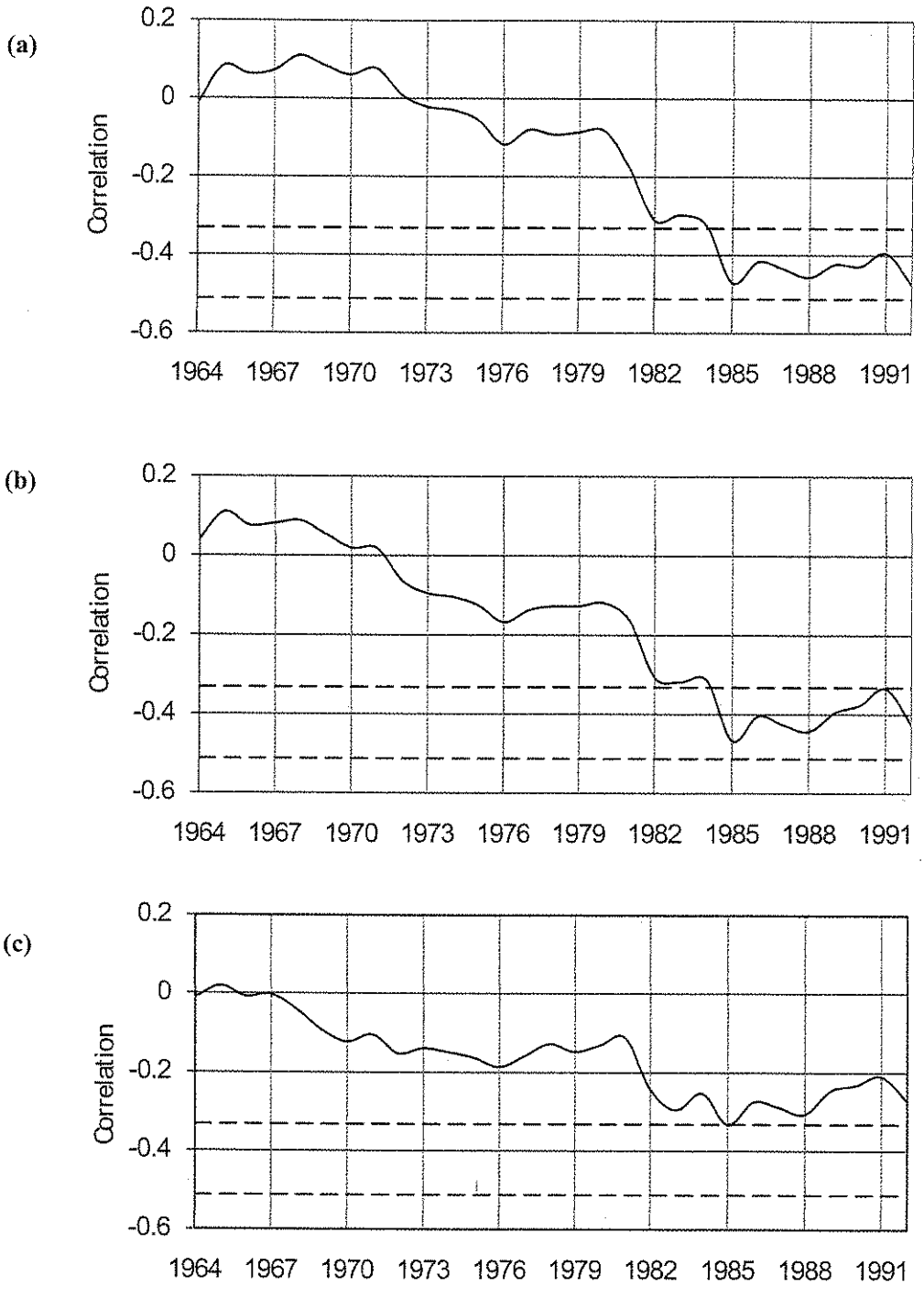

Figure 5-3 Correlation between SLP (SMH-SC) and air temperature in South China for unfiltered data in a 31-year moving window: (a) NCEP gridded region 1; (b) region 2 and (c) region 3, where the 0.05 level of significance is represented by the black dotted line, the 0.01 level of significance is represented by the grey dotted line.

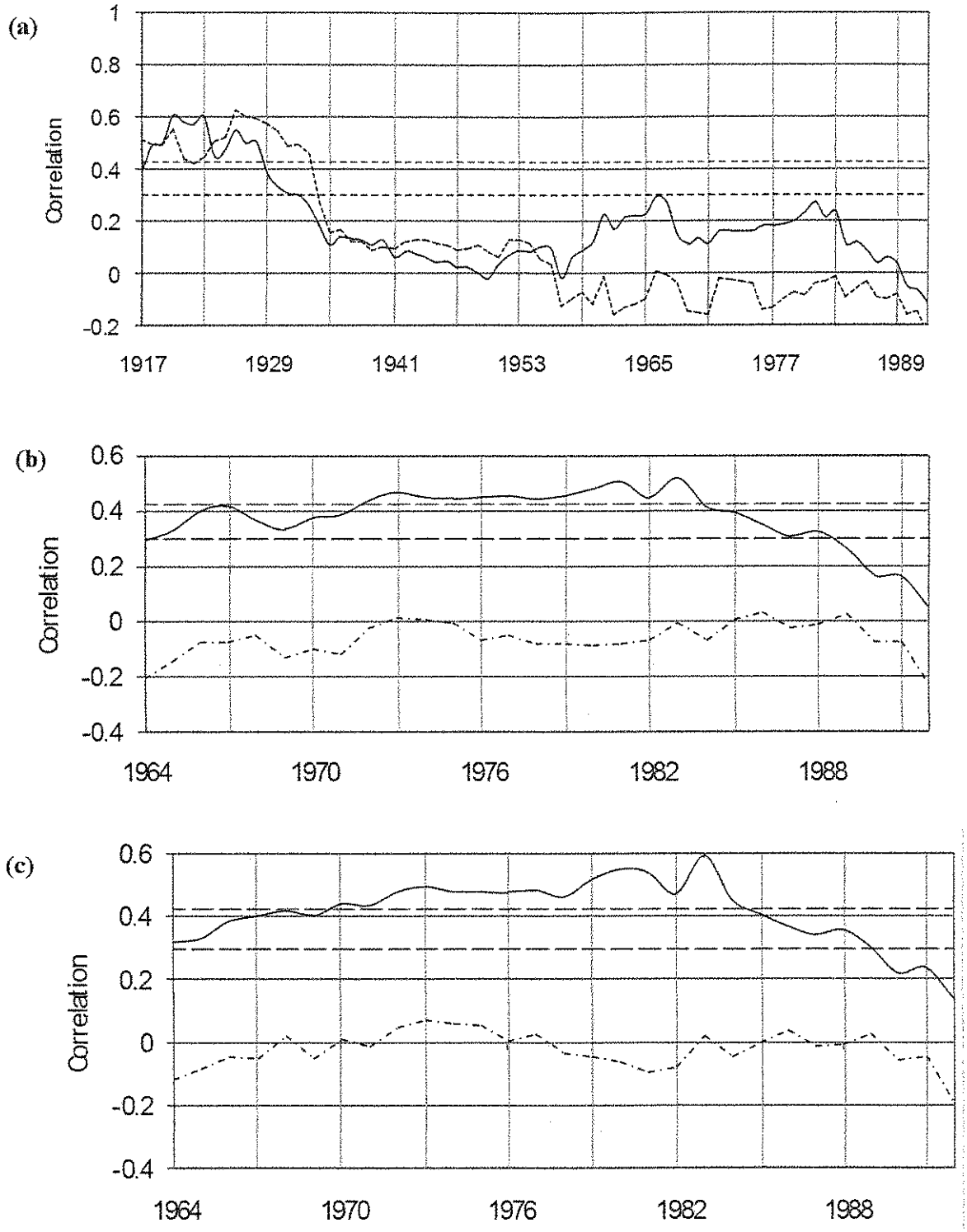

Figure 5-4 Correlation between ENSO (solid line)/PDO (dotted line) and temperature in South China for unfiltered data in a 31-year moving window: (a) Macao; (b) NCEP gridded region 2 and (c) NCEP gridded region 3, where the 0.05 level of significance is represented by the black dashed line, the 0.01 level of significance is represented by the grey dashed line

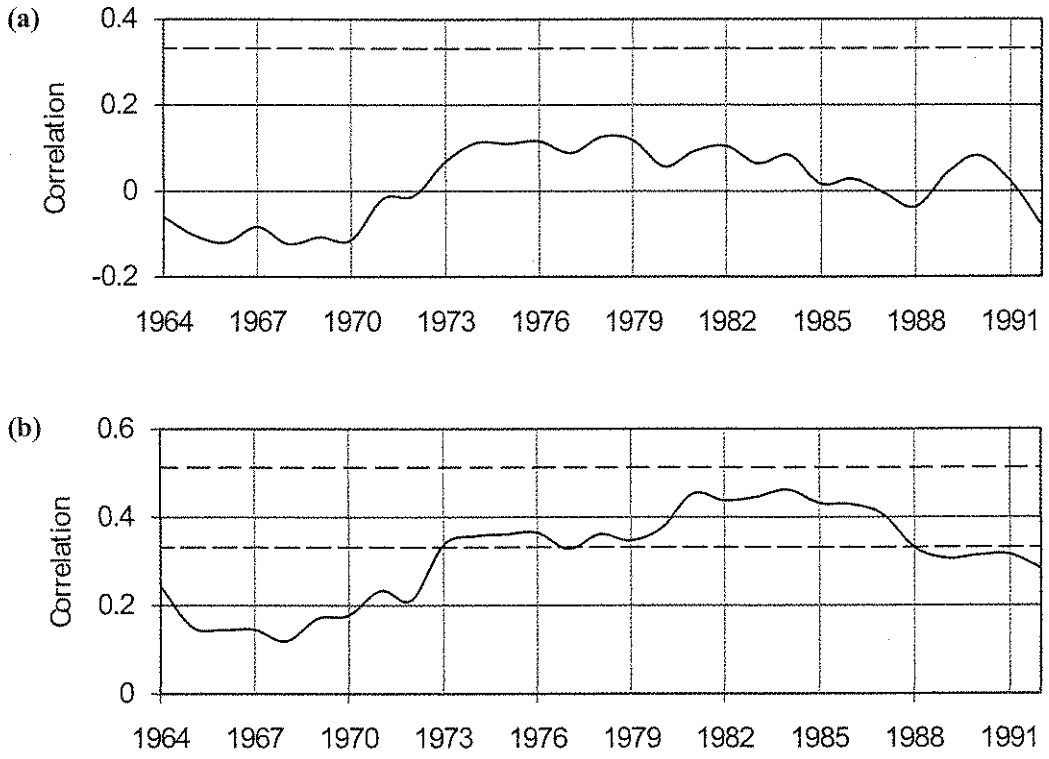

Figure 5-5 Correlation (a) between ENSO and SLP over Siberian High (b) between PDO and SLP over Siberian High for unfiltered data in a 31-year moving window, where the 0.05 level of significance is represented by the black dashed line, the 0.01 level of significance is represented by the grey dashed line

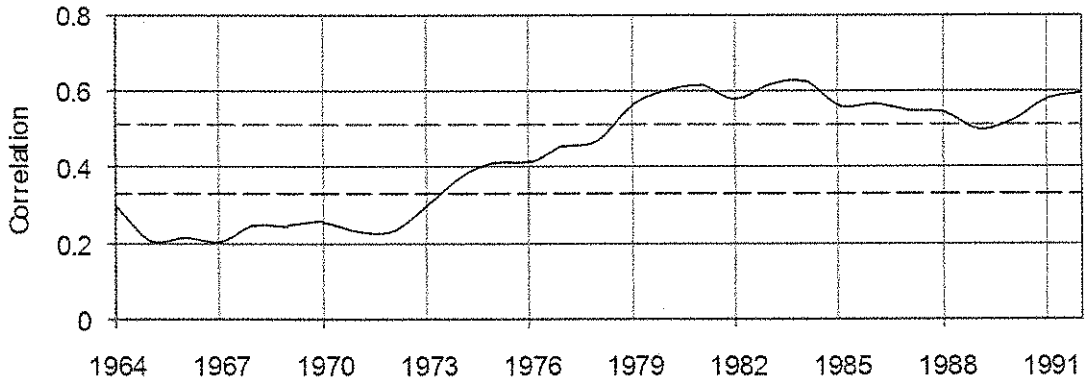

Figure 5-6 Correlation between NAO and temperature over Siberia for unfiltered data in a 31-year moving window, where the 0.05 level of significance is represented by the black dotted line, the 0.01 level of significance is represented by the grey dotted line

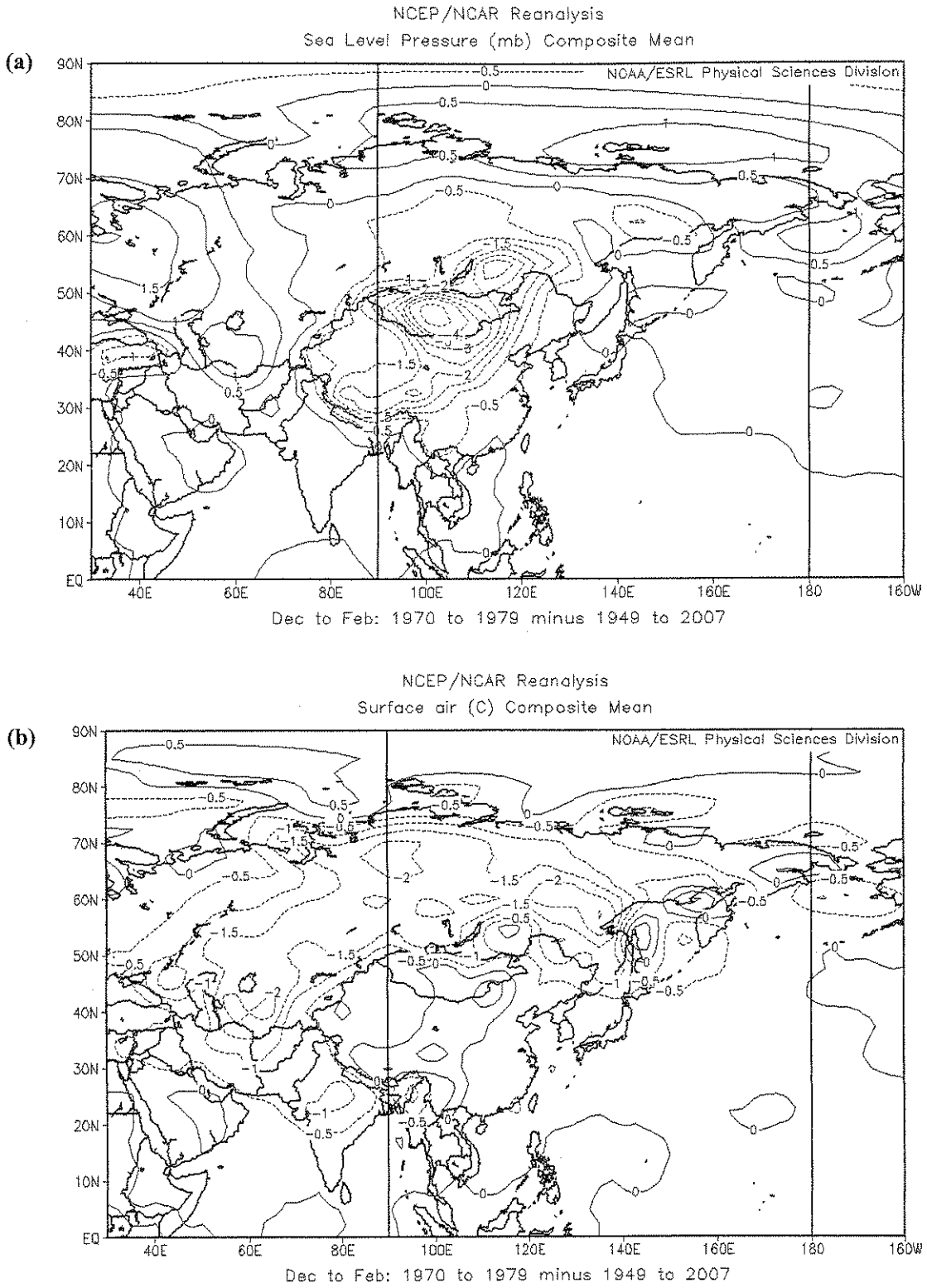

Figure 5-7 Difference in (a) SLP and (b) air temperature in East Asia in 1970-1979 with the mean in 1949-2007; contour level: 0.5 unit (NCEP/NCAR reanalysis dataset).

does. From the correlation plot with a 31-year moving window, SLP over Siberian High is positively correlated with PDO while it is weakly correlated with ENSO between early 1960s and early 2000 (Figure 5-5). The difference is probably due to the different action centers of ENSO and PDO. The intensity of Siberian High is partly affected by its difference in SLP with that in Aleutian Low. Since the SLP over Aleutian Low is affected by the phase of PDO, teleconnections might exist between the intensity of Siberian High and PDO.

Fourthly, NAO does not have correlation with temperature over South China (not shown), but it has correlation with temperature over Siberian High after 1970s (Figure 5-6). NAO, on the other hand, has low correlation with SLP over Siberian High (not shown). Since different phase of NAO results in surface westerlies anomaly blown from North Atlantic Ocean to Eurasian continent, it would affect the cold air intensity over Siberia during winter if the phase persists for long time. Hence, NAO has higher correlation with the temperature over Siberia than the SLP over there.

The possible mechanisms for the continent part and ocean part of South China may be different. On one hand, Siberian High might be responsible for the teleconnections between winter monsoon of South China in the continent part with the PDO and NAO. The strength of winter monsoon of the continent part of South China sometimes has a positive correlation with the SLP difference between Siberia and South China, SLP (SMH-SC). When SLP (SMH-SC) is large, the strength of winter monsoon might be stronger than normal and the temperature might be lower than normal, and vice versa.

Furthermore, the SLP over Siberian High always has a positive correlation with the PDO since 1949. As PDO exhibits interdecadal variation, the SLP would change on decadal timescales. Then, the winter monsoon of the continent part of South China would also exhibit interdecadal variation. The mechanism connecting Siberian High and PDO can be explained by the SLP difference between Siberian High and Aleutian Low. When PDO is positive, the air temperature would be lower in Aleutian Low and the warm-core Low intensifies. The SLP gradient between Siberian and Aleutian Low would increase, "motivating" the intensification of the Siberian High such that the cold air is brought away from it. On the contrary, the Siberian High would be weaker when the PDO is in negative phase because of the smaller SLP gradient between the High and the Low.

Moreover, Siberian High might have teleconnections with NAO. Indeed, NAO may not directly affect the intensity of Siberian High as PDO does. Previous studies found that strong NAO phase might affect the temperature in Siberian High. In particular, cold air was expected to bring to Siberia during 1960s and 1970s because of the strong negative NAO phase. When there was more cold air accumulated over Siberia, we might expect that Siberian High would intensify. However, it has just mentioned that the intensity of SMH has a positive correlation with the PDO. PDO was in negative phase during that time, so the SLP gradient between Siberia and Aleutian Low was below-normal during this period (Figure 5-7a). That would explain the reason for a below-normal Siberian High during 1970s despite the air temperature over Siberia was below-normal (Figure 5-7b).

On the other hand, the ocean part of South China is less affected by the cold surge originating from Siberian High. It might have higher correlation with ENSO than PDO. The ocean covers the major part of NCEP gridded region 2 and the whole region 3. Note that length of the NCEP gridded dataset is 59 years only (1949-2007), so their variation before 1950s cannot be determined. Between 1950s

and 2000s, the temperatures of the two regions are usually positively correlated with ENSO and have no correlations with PDO. More precisely, their positive correlations with ENSO increase from 1950s to middle 1980s and decreases significantly afterwards. There is a tri-decade negative phase between middle 1950s and late 1980s for the two regions and a positive phase since early 1990s (Figure 5-2). The temperature of South China Sea might show a large positive correlation with La Niña events and a weak correlation with El Niño events.

During La Niña events, the equatorial Pacific has stronger easterlies than normal conditions. These would result in stronger southeasterly in South China Sea. More upwelling cold water would cool the water surface, and hence the air temperature would reduce. Conversely, the southeasterly would be weak in South China Sea during El Niño events. The air temperature over the ocean would be less affected by the equatorial Pacific Ocean, so the correlation would be low in El Niño events. Since ENSO and PDO are highly correlated in the past 100 years, the correlation of NCEP gridded regions 2 and 3 with ENSO might be an evidence of interdecadal variations of the two regions. However, this conclusion is not strong because the number of samples is comparable to the period of interdecadal timescales.

5. *Summary*

This paper examines the interdecadal variations of winter monsoon over the continent part and ocean part of South China and the corresponding possible mechanisms. Air temperature is used to dictate the monsoon variation. Its most probable period on decadal timescales is found to be around 32-64 years for the continent part, which may also be true for the ocean part. However, the possible mechanisms for the two regions might be diversified. The cold surge over the continent part of South China is often related to the SLP between Siberian High and South China while the SLP over Siberian High might have teleconnections with PDO and NAO. On the other hand, there is small influence of the cold surge on the ocean part of South China and this region might have teleconnections with ENSO. However, these observations have to be verified by longer continuous and high-quality data.

Acknowledgements

The authors would like to thank NCEP for providing the monthly global reanalysis dataset (1948-2007), China Meteorological Administration, Hong Kong Observatory, Macao Meteorological and Geophysical Bureau for providing the temperature data, Joint Institute for the Study of the Atmosphere and Ocean for providing ENSO and PDO indices, Climate Research Unit, University of East Anglia, Norwich, U.K for providing NAO index and some wavelet toolkits made available by C. Torrence and A. Grinsted. This work is supported by the City University of Hong Kong research grants (7200098,7002136).

References

Chang C. P., Y. Zhang, T. Li (2000) Interannual and interdecadal variations of the East Asian summer monsoon and the tropical Pacific SSTs. Part II: Meridonal structure of the monsoon, *J. Climate*, **13**, 4326-4340.

Hurrell J. W., Y. Kushnir, G. Ottersen and M. Visbeck (2003) An overview of North Atlantic Oscillation. In: Hurrell J. W., Y. Kushnir, G. Ottersen and M. Visbeck (eds.), The North Atlantic Oscillation: Climatic significance and environmental impact, *American Geophysical Union*, Washington D.C., 7-36.

Li C. Y. (1990) Interaction between anomalous winter monsoon in East Asia and El Nino events. *Adv. Atmos. Sci.*, **7**, 36-46

Mantua N. J., S. R. Hare, Y. Zhang, J. M. Wallace and R. C. Francis (1997) A Pacific interdecadal climate oscillation with impacts on salmon production, *Bull. Amer. Meteor. Soc.*, **78**, 1069-1079.

Zhang C. D. (1996) Atmospheric intraseasonal variability at the surface in the tropical western Pacific Ocean. *J. Atmos. Sci.*, **53**, 739-758.

Zhou W., X. Wang, T. J. Zhou, C. Li & J. C. L. Chan (2007) Interdecadal variability of the relationship between the East Asian winter monsoon and ENSO, *Meteor. Atmos. Phys.*, **98**, 283-293.